Derivation of the heat capacity anomaly at a first-order transition by using a semi-adiabatic relaxation technique

2009 J. Phys.: Condens. Matter 21 075403

(http://iopscience.iop.org/0953-8984/21/7/075403)

J. Phys.: Condens. Matter **21** (2009) 075403 (5pp) doi:10.1088/0953-8984/21/7/075403

Derivation of the heat capacity anomaly at a first-order transition by using a semi-adiabatic relaxation technique

Vincent Hardy, Yohann Bréard and Christine Martin

Laboratoire CRISMAT, ENSICAEN, Université de Caen, CNRS, 6 Boulevard Maréchal Juin, F-14050 Caen 4, France

Received 13 October 2008
Published 29 January 2009
Online at stacks.iop.org/JPhysCM/21/075403

Abstract

This paper deals with the problem of determining the heat capacity anomaly associated with a first-order transition when using relaxation calorimetry. A method of data recording and analysis is proposed, which is shown to be well suited to investigate such a feature, including its hysteretical character. This technique is applied to spinel vanadates, allowing us to shed light on a recent controversy about the double-transition which takes place in these oxides.

1. Introduction

Among the various methods to measure the heat capacity of solids, the semi-adiabatic relaxation technique (also referred to as the heat-pulse technique hereafter) is one of the most widely used nowadays. In this method, a heating power P can be applied to a sample having a weak and controlled thermal link to the environment. Each measurement consists of two steps, namely a heating branch corresponding to $P \neq 0$, which is immediately followed by a cooling branch ($P = 0$) along which the temperature relaxes toward its initial value. Analyzing the thermal response of the sample along this heat pulse allows its heat capacity to be determined.

This technique is both fast and accurate for not too high temperatures (typically for $T < 200$ K), but some problems can rise when dealing with first-order transitions (FOT). Indeed, this type of transition is characterized by a series of features (latent heat, steepness of the transition, hysteresis) which can make the use of the heat-pulse technique difficult. In practice, it was already noticed that this type of calorimetry can substantially underestimate the height of the FOT peak present on the $C(T)$ curve [1, 2].

Recently, controversial results possibly related to such problems have been reported about the heat capacity of MnV_2O_4. In this spinel oxide, there are two transitions very close to each other: a ferrimagnetic second-order transition (SOT) at $\simeq$56 K and a magnetostructural FOT about 1 or 2 K below [3–10]. Two recent heat capacity studies (both carried out with the same commercial device based on a semi-adiabatic relaxation method) have reported contradictory results about the respective heights of the peaks associated with each of these transitions [6, 10]. This striking discrepancy motivated us to reinvestigate in detail the derivation of C data by this technique. The apparatus used in both cases was the heat capacity option of the Physical Properties Measurement System (PPMS) from Quantum Design (QD).

In this type of measurement, the sample is pasted with conductive grease on a platform which contains a heater (to deliver a power P) and a thermometer (to measure T_p). This platform is connected to the base temperature of the system (T_{out}) via wires which ensure a calibrated heat leak (thermal conductance K_w). After stabilization at the initial temperature T_i, the sample is heated to $T_i + T_{rise} = T_f$ by application of the heating power P (heating branch). Then, P is shut down and T goes back to T_i (cooling branch). The temperature of the platform (T_p) is monitored throughout both branches of the heat pulse.

The QD analysis is based on a sophisticated model (the so-called 2τ model) in which the heat transfer between the platform and the sample is explicitly taken into account, leading us to distinguish T_p from the temperature of the sample T_s. Accordingly, the whole system is driven by two coupled equations:

$$P = C_{ad}\frac{dT_p}{dt} + K_w(T_p - T_{out}) + K_g(T_p - T_s) \quad (1.1)$$

$$0 = C\frac{dT_s}{dt} + K_g(T_s - T_p). \quad (1.2)$$

C_{ad} is the heat capacity of the addenda (i.e. platform and grease), while C is the heat capacity of the sample itself; K_w and K_g are the thermal conductances of the wires

connecting the platform to the base temperature and of the grease, respectively. The raw data $T_p(t)$ is analyzed via the 'curve fitting method' developed by Hwang *et al* [11]. Experimentally, the main parameters that can be chosen for the measurements are the temperature rise T_{rise} and the duration of the heat pulse Δt (in the QD system, this duration is specified in terms of the approximate relaxation time of the system). There are rules to be obeyed about the T_{rise} value, especially around a transition. First, T_{rise} should be smaller than the width of the anomaly under investigation, since C is assumed to be constant over the T range scanned along the heat pulse. Second, in the presence of hysteresis—as is most often encountered for FOT—T_{rise} must also be smaller than the spacing between adjacent data points, in order to make sure there is no overlap between the temperature intervals scanned in successive measurements. For very sharp FOT, the assumption that C is constant over a temperature range equal to T_{rise} can be inappropriate. An alternative approach to deal with such a case has been proposed by Lashley *et al* [1]. These authors showed that a sharp peak on $C(T)$ can be better investigated by analyzing 'point-by-point' the time dependence of the relaxation along the cooling branch.

In MnV_2O_4, the situation is made particularly complex by the proximity between the FOT and the SOT, which leads to a superimposition of their signatures on the $C(T)$ curves. For the present study, we thus decided to consider also substituted samples of the series $Mn_{1-x}Zn_xV_2O_4$, for which it was shown that the two transitions can separate from each other while being shifted to lower temperatures [4]. Our study was mainly focused on the compound $Mn_{0.95}Zn_{0.05}V_2O_4$. This Zn content is large enough to clearly distinguish the FOT from the SOT, while being small enough to assume that the comparison of the signatures of these two types of transition should be relevant to the case of the unsubstituted MnV_2O_4.

2. Experimental details

The polycrystalline $Mn_{1-x}Zn_xV_2O_4$ samples ($x = 0$ and 0.05) were prepared by using a standard solid state reaction at high temperature. Powders of ZnO, MnO and V_2O_3 were weighted in stoichiometric ratio, mixed, ground and pressed into the shape of bars. They were then put in Pt crucibles and sealed in evacuated silica ampoules that were heated at 1100 °C for 12 h.

The obtained compounds were analyzed by x-ray diffraction (XRD) and transmission electron microscopy at room temperature. Energy-dispersive x-ray spectroscopy performed on numerous crystallites of each compound confirmed the nominal cationic compositions. Both XRD and electron diffraction patterns are characteristic of cubic spinels, exhibiting the $Fd\bar{3}m$ space group, as previously reported [12]. A small decrease of the a parameter with the Zn substitution is observed, from 0.852 12(1) nm for $x = 0.05$ to 0.85255(1) nm for $x = 0$, in agreement with the smaller size of Zn^{2+} (0.074 nm) as compared to Mn^{2+} (0.080 nm).

Magnetization measurements were performed by using an extraction technique in a PPMS (QD). The heat capacity data were recorded in the same apparatus, using a semi-adiabatic relaxation technique that is discussed in detail in section 3.

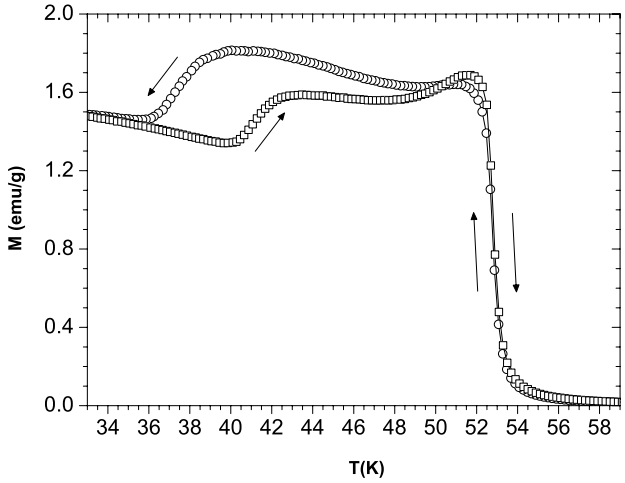

Figure 1. Magnetization curves of $Mn_{0.95}Zn_{0.05}V_2O_4$ measured upon cooling and upon warming (see arrows) in 25 Oe.

3. Results and discussion

Magnetization measurements were recorded as a function of temperature in a low-field value (25 Oe). To investigate the presence of hysteresis, $M(T)$ curves were recorded upon cooling and upon warming (see figure 1). One observes at $\simeq$52.8 K the reversible ferrimagnetic transition (SOT), while the second transition at lower temperatures is strongly hysteretic (FOT), being centered at $\simeq$41.25 K upon warming and $\simeq$37.5 K upon cooling.

In a first step, we recorded the zero-field $C(T)$ curve of $Mn_{0.95}Zn_{0.05}V_2O_4$ by using the standard analysis of the QD PPMS system. The main panel of figure 2 shows the results obtained using a small T_{rise} of 0.5%, which is *a priori* best suited to investigate sharp anomalies. While one observes a well-shaped lambda-like anomaly associated with the SOT, the signature of the FOT around 41 K is surprisingly much less pronounced.

Investigating this FOT region in more detail, we found that the heat capacity derived from the standard analysis depends a lot on the values of the measuring parameters. In particular, we observed that a clear peak rises at the FOT when the T_{rise} is increased (see the inset of figure 2). Such a drastic influence of the measuring parameters is a first clue casting doubts on the validity of the method. Moreover, this trend is even qualitatively opposed to the averaging effect that could be expected, since increasing the temperature span at each measurement should rather smooth the peak. Thus, the observed behavior clearly points to the inadequacy of the standard analysis around the FOT.

We argue that one of the main reasons for this problem is that the QD analysis is based on a fitting of both the heating and cooling branches. Since an FOT is generally accompanied by hysteresis, it is clear that analyzing both branches together is not favorable for getting reliable results. If this hysteresis is larger than T_{rise}, one can even anticipate that the presence of the FOT on the heating branch implies its absence on the cooling one. As a general rule, one can thus state that the analysis of

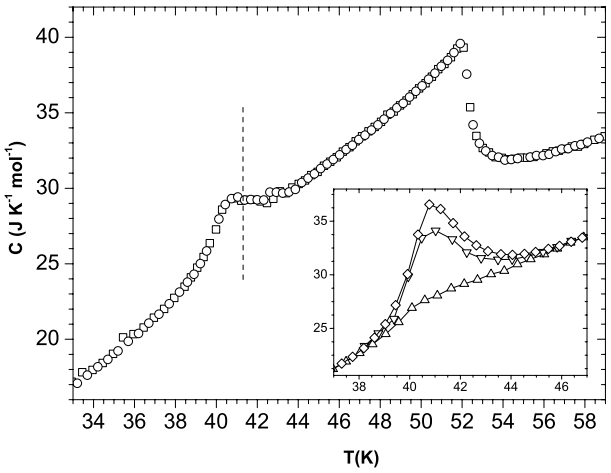

Figure 2. Heat capacity of $Mn_{0.95}Zn_{0.05}V_2O_4$, derived from the QD 2τ analysis of measurements recorded upon warming. In the main panel, the circles and squares correspond to two independent series of measurements. The dashed line indicates the transition temperature of the FOT found in the magnetization curve recorded upon heating. The inset displays the influence of the $T_{\rm rise}$ value around this FOT: triangles up (1%), triangles down (2%) and diamonds (3%).

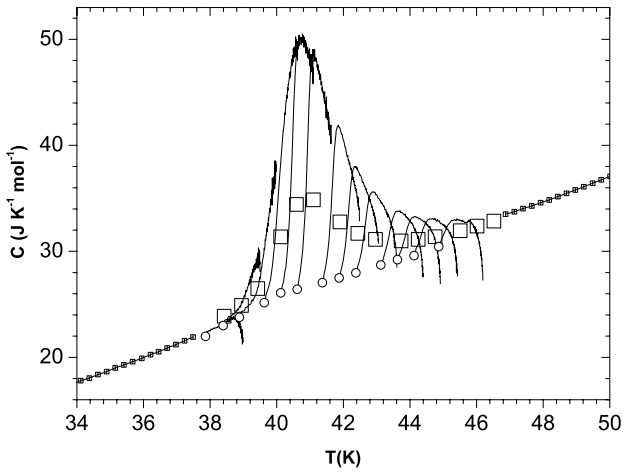

Figure 3. Heat capacity data of $Mn_{0.95}Zn_{0.05}V_2O_4$ around the FOT. The solid lines are derived from the point-by-point analysis of heating branches with equation (3.2) (the open circles highlight the starting points of each of these branches). The open squares denote the corresponding C values derived from the QD analysis. The solid squares belong to the $C(T)$ curve derived from the QD analysis over a wider T range.

the heating and cooling branches must be performed separately when investigating an FOT.

For this purpose, one needs to go back to the raw data (i.e. the $T_{\rm p}$ and P values as a function of time) and use a modelization applicable to each of the two branches. Let us consider a simplified picture in which the temperature of the sample is assumed to be equal to that of the platform, i.e. $T_{\rm s} = T_{\rm p} = T$ (the so-called 1τ model), leading to the unique equation

$$P = (C + C_{\rm ad})\frac{{\rm d}T}{{\rm d}t} + K_{\rm w}(T - T_{\rm out}), \qquad (3.1)$$

which allows $C(T)$ to be directly determined from

$$C(T) = \left\{\frac{P(T) - K_{\rm w}(T)\,[T - T_{\rm out}]}{({\rm d}T/{\rm d}t)\,(T)}\right\} - C_{\rm ad}(T). \qquad (3.2)$$

The approximation used in equation (3.1) requires an excellent thermal coupling which can be obtained in practice by using a thin and flat sample embedded in a small amount of Apiezon N grease. The achievement of such a good coupling in the present study was shown by the small difference observed between the results of the 1τ and 2τ versions of the QD analysis outside the FOT region (less than 1%).

Note that the analysis of the relaxation branch proposed by Lashley *et al* [1] corresponds to equation (3.2) with $P = 0$. It must be pointed out that the successful analysis of the relaxation branch reported by these authors was performed on a compound (Sm_2IrIn_8) in which the FOT has the peculiarity of showing almost no hysteresis [13]. We emphasize that equation (3.2) is more general since it can deal with FOT accompanied by large hysteresis, a situation for which the transition may be present only on the heating branch. Equation (3.1) shows that $T_{\rm out}$ corresponds to the stabilization temperature before the beginning of the heat pulse (in practice, this temperature was approximated by T_0, the extrapolation to $t = 0$ of the first two points of the heating branch). In equation (3.2), $K_{\rm w}(T)$ and $C_{\rm ad}(T)$ are derived from the addenda measurement which is performed before the sample is pasted onto the grease.

As a first test of equation (3.2), we investigated the whole FOT region between 38 and 46 K with measurements recorded each 1 K. The heat pulses were performed with $T_{\rm rise} = 3\%$ and $\Delta t = 5\tau$, leading to $T_{\rm f} - T_{\rm i} \simeq 1.3$ K. To avoid overlapping of the scanned temperature ranges in consecutive measurements, the complete set of data was registered in three series, each of them starting from 38 K and having a 1.8 K spacing. The results of the analysis of the heating branches via equation (3.2) is displayed in figure 3. First of all, one observes that equation (3.2) can lead to C values much larger than those derived from the standard analysis. However, the $C(T)$ profile extracted from each heating branch reveals two main problems: (1) first, each of these $C(T)$ 'traces' starts from a low value at $T \simeq T_{\rm i}$ (see the circles in figure 3) and then exhibits a sudden rise. The striking inconsistency between the data of adjacent measurements shows that the C values, in this regime, are wrong; (2) most of these $C(T)$ traces show a divergence approaching $T_{\rm f}$, which is also unphysical.

Let us address the origin of these two problems:

(1) The large C values that are normally found within a FOT reflect the latent heat present at the transition. Along the phase transformation, this heat is absorbed upon heating while it is liberated upon cooling. In our case, the low C values observed at the beginning of each heating branch suggest that the latent heat around $T_{\rm i}$ is probably absorbed during the stabilization time which precedes the heat pulse, a stage of the measurements along which there is no data recording. In this picture, a large enough departure from $T_{\rm i}$ is required to proceed with the phase transformation and thus re-incorporate the FOT latent heat in the *instantaneous* C values derived from

equation (3.2). Therefore, the initial C values of every heating branches rather reflect the background curve, i.e. the base line upon which the peak of the FOT is supposed to take place. As T is increased, the sudden rise of each $C(T)$ trace corresponds to the crossover regime where C starts being sensitive to the FOT. One may speculate that the peak on each $C(T)$ trace should reflect the true heat capacity, but the boundaries of such a reliable regime cannot be precisely defined. Qualitatively, we emphasize that this overall profile of the instantaneous $C(T)$ traces can well explain the increase of the heat capacity values derived from the standard analysis when $T_{\rm rise}$ is increased, since such values are actually averaged between $T_{\rm i}$ and $T_{\rm f}$.

(2) The second problem is the divergence of each $C(T)$ profile when approaching $T_{\rm f}$. In the thermal model of equation (3.1), $T_{\rm out}$ is by definition the equilibrium temperature when $P = 0$. Thus it is equal to T_0 at the beginning of the heating branch, while long-time relaxations showed us that T also tends to T_0 at the end of the cooling branch. However, one might consider that $T_{\rm out}$ can slightly depart from T_0 when a large amount of heat is evacuated via the wires over a short period of time, leading to a shift expected to increase with the temperature rise, i.e. $(T - T_0)$. As the simplest way to account for such a correction, let us consider a temperature dependence of $T_{\rm out}$ of the form $T_0 + y(T - T_0)$ with $y \geqslant 0$. Re-injecting this relationship in equation (3.2), the $C(T)$ can be derived from the heat-pulse data via the formula

$$C(T) = \left\{ \frac{P(T) - K_{\rm w}(T)(T - T_0)(1 - y)}{({\rm d}T/{\rm d}t)(T)} \right\} - C_{\rm ad}(T). \tag{3.3}$$

Importantly, the y value can be experimentally evaluated by considering the saturation regime on the heating branch. In this case ${\rm d}T/{\rm d}t$ tends to zero at $T = T_{\rm max} (\approx T_{\rm f})$, in such a way that equation (3.1) leads to $T_{\rm max} - T_{\rm out}(T_{\rm max}) = P(T_{\rm max})/K_{\rm w}(T_{\rm max})$. Combining with the relationship $T_{\rm out}(T_{\rm max}) = T_0 + y(T_{\rm max} - T_0)$, one obtains

$$y = 1 - [P(T_{\rm max})/K_{\rm w}(T_{\rm max})]/(T_{\rm max} - T_0). \tag{3.4}$$

It is found that equation (3.3) actually allows us to shift to higher temperatures the divergence of the $C(T)$ traces when using the y values derived from equation (3.4). As a result, one can observe substantial overlapping between the $C(T)$ derived from the heating branches of successive measurements. However, since C becomes extremely sensitive to the exact balance between the heating and leakage terms when ${\rm d}T/{\rm d}t$ starts being too small (see equation (3.3)), the last part of these branches must still be discarded.

Actually, the main problem remains that no reliable results can be derived from the first part of the heating branches. For this reason, one concludes that this method based on a series of heat pulses along the FOT is not appropriate to investigate this type of transition.

We thus turned to another approach based on a single heat pulse crossing the whole transition. To do so, $T_{\rm i}$ must be below the T range of the FOT while $T_{\rm rise}$ must be large enough to ensure that $T_{\rm f}$ is above this T range. With such a heat pulse being performed over quite a long period of time, it requires us to start from a very good stabilization in order to limit the problems of temperature drift. We performed such a measurement for $T_{\rm rise} \simeq 8$ K and $\Delta t \simeq 1000$ s, a characteristic time long enough to well approach the saturation on each branch. The y value estimated as described above leads to $y = 0.07$. With this value, analysis by equation (3.3) yields the data shown in the main panel of figure 4. One observes that: (i) the heating branch gives rise to a large peak typical of an FOT at $T \simeq 41$ K, in agreement with the results of magnetization; (ii) the results tend to merge with those of the standard analysis on both sides of the FOT; (iii) the cooling branch leads to a very different curve, which is close to the background curve in the highest T range, as expected due to the hysteresis of the FOT. However, this $C(T)$ tends to increase when coming back to T_0, a behavior possibly related to the influence of the FOT peak that is shifted to lower temperature upon cooling (down to about 37.5 K, according to the magnetization data of figure 1).

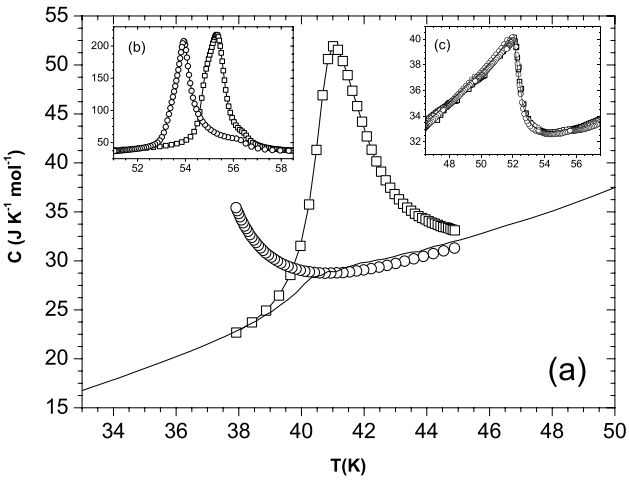

Figure 4. Heat capacity data derived from equation (3.3). The main panel (a) shows the results of a large heat pulse around the FOT in $Mn_{0.95}Zn_{0.05}V_2O_4$, derived either upon warming (squares) or upon cooling (circles). The solid line indicates the $C(T)$ curve derived from the QD analysis over a wider T range. Inset (b) shows the results of a large heat pulse around the FOT of MnV_2O_4, recorded either upon warming (squares) or upon cooling (circles). Inset (c) shows the results found around the SOT of $Mn_{0.95}Zn_{0.05}V_2O_4$, gathering data derived from the heating (squares) and cooling (circles) branches of several heat pulses.

To shed light on this issue, we re-investigated the unsubstituted MnV_2O_4 which has a smaller hysteresis [10], making it possible to scan the FOT on both heating and cooling branches along the same experiment. Inset (b) of figure 4 shows the results derived from a single large heat pulse, as previously done for $Mn_{0.95}Zn_{0.05}V_2O_4$. One observes that each branch leads to a well-defined FOT peak, the one obtained upon cooling being shifted by about 1 K with respect to the one obtained upon heating[1]. This shift is in excellent agreement with the behavior evidenced by the magnetization [10], which indicates that, in the case of $Mn_{0.95}Zn_{0.05}V_2O_4$, the upturn of $C(T)$ on the cooling branch of figure 4 is most probably related to the FOT.

[1] Note that the height of these peaks is about twice as large as that previously derived from the standard QD analysis [10].

To further check the reliability of equation (3.3), we investigated the region around the SOT of $Mn_{0.95}Zn_{0.05}V_2O_4$, a transition for which there is no hysteresis and no latent heat. As shown in inset (c) of figure 4, the lambda-like shape of the SOT is well reproduced. For such a reversible transition, it can be noted that one actually observes a good superimposition between the heating and cooling branches of each measurement. In conclusion, one can state that equation (3.3) is not only suitable to investigate the FOT region but is also able to yield $C(T)$ data, outside this T range, that are as good as those obtained from the standard analysis.

Having demonstrated the reliability of the present analysis, let us turn back to the initial motivation of this work, i.e. the comparison of the FOT and SOT peaks on the $C(T)$ curve of the spinel vanadates $Mn_{1-x}Zn_xV_2O_4$. Figure 4 shows without any ambiguities that the peak of the FOT is much larger than the one of the SOT in $Mn_{0.95}Zn_{0.05}V_2O_4$. We consider this result lends support to our previous study of MnV_2O_4, in which the highest peak on the $C(T)$ of this compound was associated with the FOT [10]. As a consequence, it also reinforces the reliability of the phase diagram of [10], which substantially differs from the one previously reported in [6].

4. Conclusion

This study reports on an alternative approach to analyze the data of relaxation calorimetry, which is shown to be well suited to the investigation of first-order transitions. Applied to the double-transition existing in some vanadate spinels, this method clearly shows that the heat capacity peak related to the FOT is substantially higher than the one related to the SOT, shedding light on a recent controversy raised about this issue.

Acknowledgment

The authors acknowledge the financial support of the 'Program Interdisciplinaire ENERGIE' of CNRS (France) for this project.

References

[1] Lashley J C, Hundley M F, Migliori A, Sarrao J L, Pagliuso P G, Darling T W, Jaime M, Cooley J C, Hults W L, Morales L, Thoma D J, Smith J L, Boerio-Goates J, Woodfield B F, Stewart G R, Fisher R A and Phillips N E 2003 *Cryogenics* **43** 369
[2] Szewczyk A, Gutowska M, Dabrowski B, Plackowski T, Danilova N P and Gaidukov Y P 2005 *Phys. Rev.* B **71** 224432
[3] Plumier R and Sougi M 1987 *Solid State Commun.* **64** 53
Plumier R and Sougi M 1989 *Physica* B **155** 315
[4] Adachi K, Suzuki T, Kato K, Osaka K, Takata M and Katsufuji K 2005 *Phys. Rev. Lett.* **95** 197202
[5] Suzuki T, Katsumura M, Taniguchi K, Arima T and Katsufuji T 2007 *Phys. Rev. Lett.* **98** 127203
[6] Zhou H D, Lu J and Wiebe C R 2007 *Phys. Rev.* B **76** 174403
[7] Garlea V O, Jin R, Mandrus D, Roessli B, Huang Q, Miller M, Schultz A J and Nagler S E 2008 *Phys. Rev. Lett.* **100** 066404
[8] Chung J-H, Kim J-H, Lee S-H, Sato T J, Suzuki T, Katsumura M and Katsufuji T 2008 *Phys. Rev.* B **77** 054412
[9] Baek S-H, Choi K-Y, Reyes A P, Kuhns P L, Curro N J, Ramanchandran V, Dalal N S, Zhou H D and Wiebe C R 2008 *J. Phys.: Condens. Matter* **20** 135218
[10] Hardy V, Bréard Y and Martin C 2008 *Phys. Rev.* B **78** 024406
[11] Hwang J S, Lin K J and Tien C 1996 *Rev. Sci. Instrum.* **68** 94
[12] Plumier R 1962 *C. R. Hebd. Séances Acad. Sci.* **255** 2244
[13] Pagliuso P G, Thompson J D, Hundley M F, Sarrao J L and Fisk Z 2001 *Phys. Rev.* B **73** 054426